Realizing exactly solvable SU(N) magnets with thermal atoms

Michael E. Beverland, Gorjan Alagic, Michael J. Martin, Andrew P. Koller, Ana M. Rey, and Alexey V. Gorshkov

Phys. Rev. A **93**, 051601 — Published 6 May 2016

DOI: 10.1103/PhysRevA.93.051601

Realizing Exactly Solvable SU(N) Magnets with Thermal Atoms

Michael E. Beverland,[1] Gorjan Alagic,[2] Michael J. Martin,[1]
Andrew P. Koller,[3] Ana M. Rey,[3] and Alexey V. Gorshkov[4]

[1] *Institute for Quantum Information & Matter, California Institute of Technology, Pasadena, CA 91125, USA*
[2] *Department of Mathematical Sciences, University of Copenhagen*
[3] *JILA, NIST, and Department of Physics, University of Colorado Boulder, CO 80309*
[4] *Joint Quantum Institute and Joint Center for Quantum Information and Computer Science, NIST/University of Maryland, College Park, MD 20742*

We show that n thermal fermionic alkaline-earth atoms in a flat-bottom trap allow one to robustly implement a spin model displaying two symmetries: the S_n symmetry that permutes atoms occupying different vibrational levels of the trap and the SU(N) symmetry associated with N nuclear spin states. The symmetries makes the model exactly solvable, which, in turn, enables the analytic study of dynamical processes such as spin diffusion in this SU(N) system. We also show how to use this system to generate entangled states that allow for Heisenberg-limited metrology. This highly symmetric spin model should be experimentally realizable even when the vibrational levels are occupied according to a high-temperature thermal or an arbitrary non-thermal distribution.

PACS numbers: 34.20.Cf, 06.30.Ft, 67.85.-d, 75.10.Jm

The study of quantum spin models with ultracold atoms [1, 2] promises to give crucial insights into a range of equilibrium and non-equilibrium many-body phenomena from quantum spin liquids [3] and many-body localization [4] to quantum quenches [5–7] and quantum annealing [8]. While other approaches exist [9–12], the most common approach to implement a quantum spin model with ultracold atoms relies on preparing a Mott insulator in an optical lattice, where the internal states of atoms on each site define the effective spin [1, 13–19]. Virtual hopping processes to neighboring sites and back then give rise to effective superexchange spin-spin interactions. Since the superexchange interactions are typically very weak ($\ll$ kHz) [1] (unless the traps are operated near surfaces, which can reduce spacings and increase energy scales [20–22]), it is a significant challenge in experimental cold atom physics to achieve temperatures and decoherence rates low enough to access superexchange-based quantum magnetism.

Since ultracold atoms can be prepared in specific internal (i.e. spin) states with extremely high precision, spin temperatures that can be realized are much lower than the experimentally achievable motional temperatures. It is therefore tempting to circumvent the problem of high motional temperature by constructing a spin model in such a way that the motional and spin degrees of freedom are effectively decoupled. We provide a recipe for such a decoupling and hence for realizing spin models with thermal atoms.

The first crucial ingredient for implementing such a spin model is to depart from second-order superexchange interactions and use contact interactions to first order [23–32]. As shown in Fig. 1(a), this can be achieved if all atoms sit in different orbitals of the same anharmonic trap and remain in these orbitals throughout the evolution, which is a good approximation for weak interactions [23–25, 30, 31]. In that case, the occupied orbitals play the role of the sites of the spin Hamiltonian. However, because of high motional temperature in such systems, every run of the experiment typically yields a different set of populated orbitals and hence a different spin Hamiltonian [30]. Thus, unless the dynamics are constrained to states symmetric under arbitrary exchanges of spins [30], every run of the experiment would lead to different spin dynamics.

The second crucial ingredient to decouple spin and motion is therefore to use an infinite one-dimensional square-well potential as the anharmonic trap, with the motion frozen along the other two directions. The interaction terms in the spin Hamiltonian H are proportional to the squared overlap of pairs of distinct sinusoidal orbitals, and are thus all of equal strength. Therefore $\hat{H}$ is independent of which orbitals are occupied, leading to spin-motion decoupling and temperature independent predictions, as well as opening up the possibility of precise control. Moreover, since $\hat{H}$ is invariant under any relabeling of the n occupied orbitals, $\hat{H}$ has S_n permutation symmetry.

Alkaline-earth atoms enrich the symmetry. In such

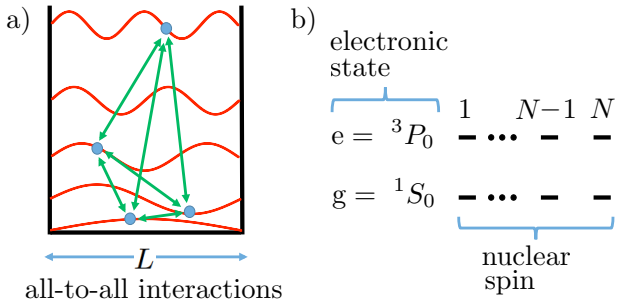

FIG. 1: (a) Contact interactions between atoms in the orbitals of a one-dimensional infinite square well of width L are all-to-all with equal strength. (b) With nuclear spin I, each of the electronic clock states g and e of fermionic alkaline-earth atoms can offer N degenerate states, with $N \leq 2I + 1$.

atoms, the vanishing electronic angular momentum J in the electronic clock states $g = {}^1S_0$ and $e = {}^3P_0$ results in the decoupling of the nuclear spin I from J [Fig. 1(b)]. This endows $\hat{H}$ with an additional $SU(N)$ spin-rotation symmetry, where N can be tuned between 2 and $2I+1$ by choosing the initial state [33–38]. Restricted to g, $\hat{H}$ is just the sum of spin-swaps over all pairs of occupied orbitals and can be diagonalized in terms of irreducible representations of the group of symmetries $G = S_n \times SU(N)$.

Motional-temperature-insensitive spin models can also be realized using long-range interactions between ions in Paul traps [39], Penning traps [6, 7, 40], and also between molecules [41–44] or Rydberg atoms [12] pinned at different sites of an optical lattice. However, the realization of $SU(N)$-symmetric spin models in such systems requires a great deal of fine tuning [45].

Motivated by the exploration of how quantum systems evolve after quantum quenches and whether (or how) they equilibrate and/or thermalize [46], especially in the presence of long-range interactions [6, 7], we first study spin diffusion [44, 47, 48] in a system of g atoms only. Due to crucial use of representation-theoretic techniques, our calculations are not only exponentially faster than naive exact diagonalization but also, for $N = 2$, yield a closed-form expression for all n. We then present a protocol that employs both g and e states to create Greenberger-Horne-Zeilinger (GHZ) states [49], which could be used to approach the Heisenberg limit for metrology and clock precision [50].

Spin Hamiltonian. A single mass-M fermionic alkaline-earth atom (for now, in its ground electronic state g) trapped in a 1D spin-independent potential $V(x)$ has real orbitals $\phi_j(x)$ with energies E_j satisfying $\left[-(\hbar^2/2M)\partial^2/\partial x^2 + V(x)\right]\phi_j(x) = E_j\phi_j(x)$. The operator $\hat{c}^\dagger_{jp}$ creates an atom from the vacuum in $\phi_j(x)$ with nuclear spin state $p \in 1, 2, ..., N$. For n identical atoms in the same potential with contact s-wave interactions, the Hamiltonian is $\hat{H} = \sum_{jp} E_j \hat{c}^\dagger_{jp}\hat{c}_{jp} + \sum_{p<q}\sum_{jkj'k'} U_{jkj'k'}\hat{c}^\dagger_{jp}\hat{c}_{j'p}\hat{c}^\dagger_{kq}\hat{c}_{k'q}$, where $U_{jkj'k'} = 4\pi\hbar\omega_\perp a_{gg}\int_{-\infty}^{\infty} dx \phi_j(x)\phi_k(x)\phi_{j'}(x)\phi_{k'}(x)$, a_{gg} is the 3D-scattering length, and a potential with frequency $\omega_\perp$ freezes out transverse motion.

To obtain the desired Hamiltonian, we specialize to a width-L infinite square well $V(x)$, with well-known eigenstates $\phi_j(x) = \sqrt{2/L}\sin(j\pi x/L)$ for $0 \le x \le L$, with energy $E_j = (\pi j/L)^2/2M$. Then $U_{jkj'k'}$ is zero unless (i): $(j \pm k) = \pm(j' \pm k')$; to first order in the interaction, we can also set $U_{jkj'k'} \to 0$ unless $\sum_{jp} E_j \hat{c}^\dagger_{jp}\hat{c}_{jp}$ is conserved, which occurs when (ii): $j^2 + k^2 = j'^2 + k'^2$. Both (i) and (ii) are satisfied if and only if $(j', k') = (j, k)$ or $(k', j') = (j, k)$. As the system conserves orbital occupancies, it can be described by a spin model. Assuming orbitals are at most singly occupied ($\hat{n}_j = \sum_p \hat{c}^\dagger_{jp}\hat{c}_{jp} \le 1$ for all j) [80], the spin Hamiltonian is:

$$\hat{H} = -U\sum_{j<k}\hat{s}_{jk}, \tag{1}$$

where $\hat{s}_{jk} \equiv \sum_{pq}\hat{c}^\dagger_{jp}\hat{c}_{jq}\hat{c}^\dagger_{kq}\hat{c}_{kp}$ swaps spins j and k, and the sum is over occupied orbitals. Crucially, $U \equiv 4\pi a_{gg}\hbar\omega_\perp/L$ is independent of j and k. We dropped a constant $\sum_j E_j + n(n-1)U/2$, which will have no effect on spin dynamics. For a fixed set of occupied orbitals, $\hat{H}$ has N^n basis states $|p_1, p_2, ..p_n\rangle$ with $p_j \in 1, ..., N$.

Exact eigenenergies and eigenstates. For $N = 2$, the spin-swap can be written in terms of the Pauli operators: $\hat{s}_{jk} = 1/2 + (\hat{\sigma}^x_j\hat{\sigma}^x_k + \hat{\sigma}^y_j\hat{\sigma}^y_k + \hat{\sigma}^z_j\hat{\sigma}^z_k)/2$, allowing Eq. (1) to be written as $\hat{H} = -U\left[\vec{S}^2 + \frac{n}{4}(n-4)\right]$, where $\vec{S} = \frac{1}{2}\sum_j \vec{\sigma}_j$. The eigenstates of $\hat{H}$ for $N = 2$ are the well-known Dicke [51] states $|S, S_z, k\rangle$, with energies $E(S) = -U\left[S(S+1) + \frac{n}{4}(n-4)\right]$. The quantum number k labels distinct states with the same $\vec{S}^2$ and $\hat{S}^z$ eigenvalues. We now describe the general case for arbitrary N, but defer derivations and detailed explanation to the Supplemental Material [52].

Equation (1) has two obvious symmetries: permutations in S_n of the n occupied orbitals, and application of the same unitary in $SU(N)$ to all of the spins giving a group $G = S_n \times SU(N)$ of symmetries. From Schur-Weyl duality [53], we conclude that for each integer partition $\vec{\lambda} = (\lambda_1, \lambda_2, ..., \lambda_N)$ such that $\sum_i \lambda_i = n$ and $\lambda_{i+1} \le \lambda_i$, there is a subspace of constant energy $E(\vec{\lambda})$. The $\vec{\lambda}$-subspaces (called irreducible representations of G) are orthogonal and span the full Hilbert space.

A *Young diagram* is a pictorial representation of $\vec{\lambda}$ consisting of a row of λ_1 boxes above a row of λ_2 boxes, which is above a row of λ_3 boxes etc. It is also useful to define $\vec{\gamma} = (\gamma_1, \gamma_2, ..., \gamma_{\lambda_1})$ as the column heights of the Young diagram $\vec{\lambda}$. Figure 2(a) shows an example with $n = 7$ and $N = 3$.

To create an eigenstate in any $\vec{\lambda}$-subspace, first consider the basis state: $|T\rangle \equiv |1, 2, ..., \gamma_1\rangle\ |1, 2, ..., \gamma_2\rangle ...\ |1, 2, ..., \gamma_{\lambda_1}\rangle$, which is chosen by associating orbitals with boxes of the Young diagram as in Fig. 2(b), and putting those orbitals in spin states as in Fig. 2(c). We form $|\vec{\lambda}\rangle$ (which is one of many [52] eigenstates in the $\vec{\lambda}$-subspace) by antisymmetrizing $|T\rangle$ over orbitals associated with boxes in each column of $\vec{\lambda}$:

$$|\vec{\lambda}\rangle = |\mathcal{A}\{12...\gamma_1\}\rangle|\mathcal{A}\{12...\gamma_2\}\rangle...|\mathcal{A}\{12...\gamma_{\lambda_1}\}\rangle, \tag{2}$$

where $\mathcal{A}\{...\}$ antisymmetrizes its argument, for example: $|\mathcal{A}\{123\}\rangle = |123\rangle + |312\rangle + |231\rangle - |132\rangle - |321\rangle - |213\rangle$. The normalization constant is fixed by $\langle\vec{\lambda}|\vec{\lambda}\rangle = \gamma_1!\gamma_2!...\gamma_{\lambda_1}!$. We see that the Young diagram associates symmetry with rows and antisymmetry with columns.

From $\hat{H}|\vec{\lambda}\rangle = E(\vec{\lambda})|\vec{\lambda}\rangle$ one can prove $E(\vec{\lambda})/(-U) = \sum_{i=1}^{N}\binom{\lambda_i}{2} - \sum_{j=1}^{\lambda_1}\binom{\gamma_j}{2}$: the number of ways of choosing

two boxes in the same row of $\vec{\lambda}$, minus the number of ways of choosing two boxes in the same column [52]. This is in line with the intuition that the swap picks up $-U$ for each symmetric pair and $+U$ for each antisymmetric pair in the Young diagram. In terms of $\vec{\lambda}$,

$$E(\vec{\lambda}) = -\frac{U}{2}\sum_{i=1}^{N}(\lambda_i - 2i + 1)\,\lambda_i. \tag{3}$$

Figure 2(d) illustrates the eigenvalues and eigenstates of $\hat{H}$ for the simple case of $n = 4$ and $N = 3$, along with the corresponding Young diagrams. There is an equivalence for the $SU(2)$ case between Young diagram (λ_1, λ_2) and angular momentum quantum number S given by $S = (\lambda_1 - \lambda_2)/2 = (2\lambda_1 - n)/2$.

Spin diffusion dynamics. Spin diffusion is the process by which evolution under a generic spin Hamiltonian causes initially ordered states to diffuse [44, 47, 48]. We take initial state $|\psi(0)\rangle = |1\rangle^{\otimes m_1}|2\rangle^{\otimes m_2}...|N\rangle^{\otimes m_N}$.

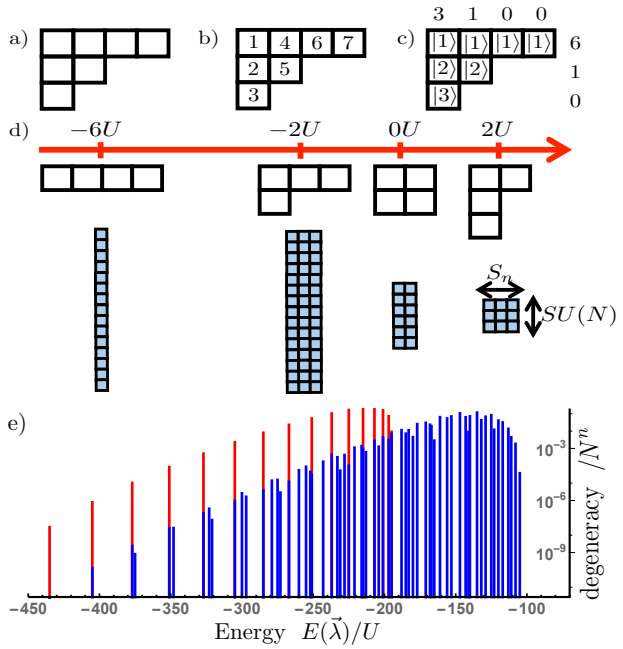

FIG. 2: (a) A Young diagram $\vec{\lambda} = (4, 2, 1)$ [with $\vec{\gamma} = (3, 2, 1, 1)$] for $n = 7, N = 3$. (b) A labeling of boxes in $\vec{\lambda}$ from 1 to n, increasing down columns, starting at the left. (c) Orbitals associated with boxes in row p are put in spin state $|p\rangle$ to form basis state $|T\rangle = |1231211\rangle$ [spins ordered as in (b)], used to construct eigenstate $|\vec{\lambda}\rangle = |\mathcal{A}\{123\}\rangle|\mathcal{A}\{12\}\rangle|11\rangle$ with $E(\vec{\lambda})/(-U) = \sum_i \binom{\lambda_i}{2} - \sum_j \binom{\gamma_j}{2} = 6+1+0-3-1-0-0 = 3$. (d) The set of all Young diagrams for $n = 4$ and $N = 3$, with energies above. Below, eigenstates are represented by colored boxes: rotations in $SU(N)$ transform between eigenstates in the same colored column, while permutations in S_n transform between eigenstates in the same colored row. Representative states are found using the prescribed construction to be $|1111\rangle$, $(|12\rangle - |21\rangle)\,|11\rangle$, $(|12\rangle - |21\rangle)(|12\rangle - |21\rangle)$, and $(|123\rangle + |312\rangle + |231\rangle - |132\rangle - |213\rangle - |321\rangle)\,|1\rangle$, respectively. (e) Spectrum for $n = 30$ with $N = 2$ (red), and $N = 3$ (blue).

Note any computational basis state can be changed to this form by reordering occupied orbitals. We consider the time evolution of observable $\hat{Q} = \sum_{j=1}^{m_1}|1\rangle_j\langle 1|_j$: the number of the first m_1 orbitals in spin-state $|1\rangle$. This is the simplest observable capturing the broken symmetry of the initial state. The expectation of $\hat{Q}$ evolves according to: $Q(t) \equiv \langle\psi(0)|e^{i\hat{H}t}\hat{Q}e^{-i\hat{H}t}|\psi(0)\rangle$, omitting $\hbar$ where convenient from here on.

Calculating $Q(t)$ for a generic Hamiltonian requires matrix diagonalization, which scales exponentially with n (for fixed N). Using the symmetry of Hamiltonian (1) and the Wigner-Eckart theorem for $SU(N)$, we obtain an explicit sum (see Eq. (S11) in Ref. [52]) for $Q(t)$ in terms of Clebsch-Gordan and recoupling coefficients. For the case of $N = 2$, with initial state of $m_1 = m$ spin up and $m_2 = n - m$ spin down orbitals, using well-known closed forms for the Clebsch-Gordan and recoupling coefficients:

$$Q(t) = m + \sum_{S=|n-2m|/2+1}^{n/2}\gamma(S)[\cos(2SUt) - 1], \tag{4}$$

where $\gamma(S) = \frac{4S^2-(n-2m)^2}{4S}\binom{n}{n/2+S}/\binom{n}{n-m}$. For $N > 2$, closed forms for the required coefficients are not known to the authors, but can be calculated efficiently using standard algorithms as in Ref. [54]. In Fig. 3, we compare the evolution of the same operator and total particle number for initial states with $N = 2$ spin states and $N = 3$ spin states. The oscillations are much less pronounced and spin diffusion occurs more fully (Q drops lower) for the latter state. With this model, looking at times away from the multiples of the revival time $2\pi/U$, one could study apparent near-equilibration of some observables (such as Q in the $N = 3$ case) acting on the first m_1 spins. Perturbations could be added to the system to remove revivals and potentially allow for the thermalization of the first m_1 spins.

GHZ state preparation. Highly entangled states could lead to short-term applications in metrology [50, 55], and long-term applications in quantum information [56, 57]. It is particularly timely to design ways for implementing entanglement-assisted – and hence more accurate – clocks with alkaline-earth atoms [58, 59] since such atoms recently gave rise to the world's best clock and have nearly approached the quantum projection noise limit for unentangled atoms [60, 61]. We now show our system offers a natural way to produce metrologically relevant entanglement (in the form of GHZ states) in alkaline-earth clock experiments. It is the experimental realization of quantum spin models in alkaline-earth clock experiments [30] and the potential application of these spin models to improve the clocks that motivated this work.

To create a GHZ state, we allow atoms in the excited electronic state e with energy ω_{eg} above the ground electronic state g [see Fig. 1(b)]. First assume $N = 2$. An applied magnetic field adds Zeeman spin-splittings $B_g \neq B_e$ [62] to both g and e states. To first order in the interac-

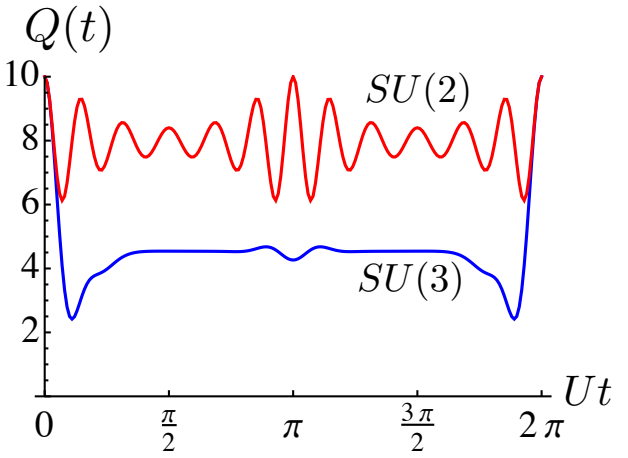

FIG. 3: Exact time evolution of $\hat{Q} = \sum_{j=1}^{10} |1\rangle_j\langle 1|_j$, which counts the number of the first ten orbitals in spin state $|1\rangle$. Two initial states are compared: $|1\rangle^{\otimes 10}|2\rangle^{\otimes 20}$ for $SU(2)$ and $|1\rangle^{\otimes 10}|2\rangle^{\otimes 10}|3\rangle^{\otimes 10}$ for $SU(3)$. The initial evolution is similar, but more $|1\rangle$ states diffuse out of the first ten orbitals for $SU(3)$ later on. Since all $E(\vec{\lambda})$ are integer multiples of U, complete revival occurs at $Ut = 2\pi$. In the $SU(2)$ case, the oscillation is dominated by the smallest S in Eq. (4). This is consistent with the fact that for fixed S_z, the size of the eigenspaces decreases with S, causing overlap to be larger with subspaces of small S generically.

tion strength, the spin Hamiltonian is [52]:

$$\hat{H} = \hat{H}_{sp} + \sum_{\alpha<\beta} U_{\alpha\beta}\left(\hat{n}_\alpha\hat{n}_\beta - \sum_{j\neq k}\hat{c}^\dagger_{j\alpha}\hat{c}_{j\beta}\hat{c}^\dagger_{k\beta}\hat{c}_{k\alpha}\right). \quad (5)$$

The single-particle Hamiltonian is $\hat{H}_{sp} = \omega_{eg}\hat{n}_e + B_g(\hat{n}_{1g} - \hat{n}_{2g}) + B_e(\hat{n}_{1e} - \hat{n}_{2e})$, the sum $\alpha < \beta$ is over distinct pairs of $1g$, $1e$, $2g$ and $2e$. Constants $U_{\alpha\beta}$ are derived in terms of (electronic-state dependent) scattering lengths [52]. Note that $\hat{n}_{1g}$, $\hat{n}_{2g}$, $\hat{n}_{1e}$ and $\hat{n}_{2e}$ are separately conserved by Hamiltonian (5). As shown in Fig. 4, to create the n-particle GHZ state $(|1g1g..1g\rangle + |2g2g..2g\rangle)$ from $|1g1g..1g\rangle$, three consecutive pulses should be applied:

1. Spatially inhomogeneous, weak, many-body $\pi/2$ pulse $e^{-i\nu_{eg}t}\sum_j \Omega_j^{eg}(|1e\rangle_j\langle 1g|_j + |2e\rangle_j\langle 2g|_j) + h.c.$ with frequency $\nu_{eg} = \omega_{eg} + (B_e - B_g) + nU_{1e1g}$.

2. Spatially uniform, weak, single-atom π pulse $e^{-i\nu_{12}t}\Omega^{12}\sum_j(|2g\rangle_j\langle 1g|_j + |2e\rangle_j\langle 1e|_j) + h.c.$ with frequency $\nu_{12} = 2B_g$.

3. Pulse 1, but for pulse area π, not $\pi/2$.

The frequency of the first pulse picks out an effective two-level system consisting of $|1g1g..1g\rangle$ and $|\{1e1g..1g\}\rangle \propto \sum_{jp}(\Omega_j^{eg} - \bar{\Omega}^{eg})|1e\rangle_j\langle 1g|_j|1g1g..1g\rangle$ (we defined $\bar{\Omega}^{eg} \equiv \sum_j \Omega_j^{eg}/n.$). The pulse must be spatially inhomogeneous to make Ω_j^{eg} j-dependent and to be able to access eigenstates with interaction-dependent energies (i.e.

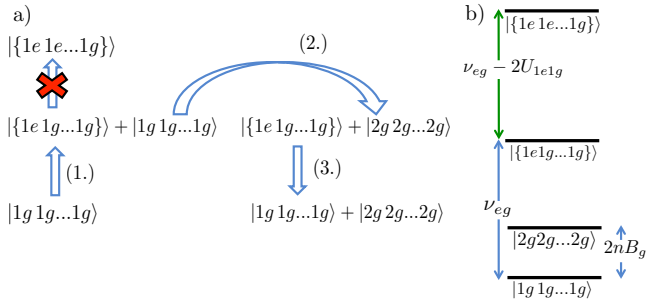

FIG. 4: (a) System prepared in $|1g1g..1g\rangle$. Spatially inhomogeneous pulse (1.) results in equal superposition of this state and $|\{1e1g..1g\}\rangle$, containing one e atom. An interaction blockade prevents coupling to states with two e atoms. Pulse (2.) flips the spins of the all-g state. The initial pulse is reversed in pulse (3.), resulting in the GHZ state. (b) Relevant energy levels of the Hamiltonian with e and g states and the magnetic field. Note that pulses (1.) and (3.), which involve states $|1g1g..1g\rangle$ and $|\{1e1g..1g\}\rangle$, do not couple to state $|\{1e1e..1g\}\rangle$ since there is a blockade of $2U_{1e1g}$. Similarly, during pulse (2.), blockade prevents excitation of $|\{1e1g..1g\}\rangle$.

not fully symmetric eigenstates). The precise form of the inhomogeneity is unimportant, as all $n-1$ non-symmetric states with a single e atom are degenerate in $\hat{H}$ due to its S_n symmetry. We use curly brackets to signify linear combinations of $|1e1g..1g\rangle$ and permutations. No state $|\{1e1e..1g\}\rangle$ is coupled by pulse 1 because the first e atom blockades the addition of another by energy $2U_{1e1g}$ [52]. The second pulse has no effect on $|\{1e1g..1g\}\rangle$ because the e atom blockades transition to any state $|\{1e2g..1g\}\rangle$. The final pulse does not affect the $|2g2g..2g\rangle$ state because the pulse is off-resonant by energy of order $(B_e - B_g)$ [52]. Note that although the precise form of the inhomogeneity in the first pulse is unimportant, the final pulse and the first pulse must have the same inhomogeneity. Since all three pulses rely on blockade, each pulse must take time $\gg 1/U$. Curiously, the fact that the interactions in our spin model have effectively infinite range makes our spins analogous to long-range interacting Rydberg atoms, for which a similar protocol exists for generating maximally entangled states [63]. We have designed the protocol to have at most one e atom at any time, which avoids the potential problem of inelastic e-e collisions [64], while g-e losses are negligible [35, 65].

For integer m such that $N \geq 2^m$, m GHZ states can be created provided one has sufficient control [66] over the nuclear spin states coupled by the pulses [52]. Several GHZ states can be used to create a single GHZ state of better fidelity via entanglement pumping [66, 67].

Experimental Considerations. We use the example of ^{87}Sr to describe how to experimentally access the physics we discuss in this work.

The key requirements of this proposal are as follows. Firstly, the x and y degrees of freedom must be frozen, forming a 1D interacting system along the z direction.

Secondly, $U = (4\pi a_{gg}\hbar\omega_\perp)/L$ should be less than the single-particle energy separations, the smallest of which is $3\hbar^2(\pi/L)^2/M$, ensuring the validity of the first-order perturbation theory in our derivation of Eq. (1). This constrains the relative sizes of L and $\omega_\perp$. Thirdly, variations in U_{jkjk}, with standard deviation ΔU, give rise to variations in eigenergies $\sim n\Delta U$ (see Supplemental Material [52]). Therefore, we also require $\Delta U/U < 1/n$.

To meet these requirements, we propose an optical lattice potential formed by two magic-wavelength (813 nm) [68] orthogonal standing waves in x and y. This could be achieved with a pair of angled beams [69] for each standing wave, in bow tie configuration [see Fig. 5].

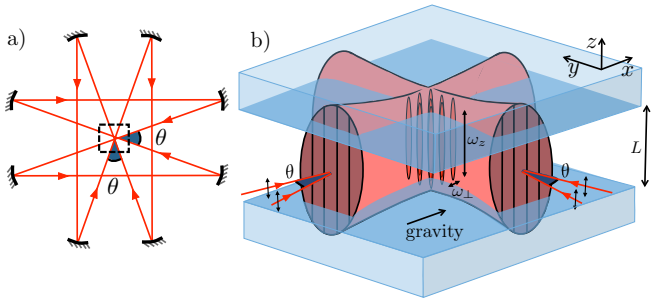

FIG. 5: Layout of suggested experimental implementation. a) A bow tie beam arrangement of two pairs of beams aimed at a vacuum chamber. In each pair, the two beams have different k vector directions of $\theta = 30^o$, forming an in-plane standing wave perpendicular to that pair's net k vector direction. The pair of perpendicular standing waves forms an attractive lattice. b) The two-dimensional lattice of attractive-potential tubes forms with transverse vibrational frequency $\omega_\perp$ and lattice constant Δx. The finite beam width results in a weak potential in the z direction with vibrational frequency ω_z. Gravity is in the beam plane to avoid a potential gradient along the tubes. Blue-detuned light outside the central region of width L forms caps for the tubes. Following the Supplemental Material [52], we obtain $\omega_\perp \simeq 2\pi \times 10$ kHz, $\Delta x \simeq 3$ μm, $\omega_z \simeq 2\pi \times 100$ Hz, and $L \simeq 10$ μm.

An additional blue-detuned optical potential at 394 nm, the Sr blue magic wavelength, is applied to form approximate 1D square wells from the resulting tubes. The potential could be formed from a projected image of a Gaussian beam with waist 30 μm and total power 400 mW screened in the center by a rectangular mask of width $L = 10$ μm. Imperfect cap potentials, along with a finite curvature of the flat potential, contribute to ΔU and are analyzed in the Supplemental Material [52].

With these parameters, and $a_{gg} = 5.1$ nm [70], one obtains $U/\hbar = (4\pi a_{gg}\omega_\perp)/L \approx 2\pi \times 10$ Hz, and should be able to meet all three of the aforementioned key requirements with $\lesssim 20$ atoms in a single tube. Further details are included in the Supplemental Material [52]. Such values of $U_{\alpha\beta} \sim U$ [35] can potentially allow for the preparation of the GHZ state on a time scale comparable to the ~ 1s experimental cycle time for state-of-the-art clocks [60], and may thus provide a practical advantage over the use of unentangled atoms.

To observe spin diffusion, the initial state could be formed by cooling a spin-polarized system to the limit where the lowest n orbitals are occupied. One could potentially consider taking advantage of large N for better cooling [71, 72]. One coud address different orbitals either spatially with spin-changing pulses which only couple to certain orbitals (for example using pulses focused on the center of the well and hence decoupled from orbitals that vanish there), or energetically by temporarily transferring atoms to another electronic state subject to a different potential. To observe spin diffusion with thermal atoms, one could rely on the fact that about half of the occupied orbitals are odd, and the other half are even, which becomes statistically more accurate for larger n. It is possible to address only the even orbitals by using a beam focused at the center of the well, since the odd orbitals vanish there. This could be extended to larger N by using additional beams focused on other points in the well.

Outlook. The proposed system opens a wide range of research and application avenues beyond those discussed above. For the case of $N = 2$, our $S_n \times SU(N)$-symmetric Hamiltonian can be used for decoherence-resistant entanglement generation [73], a method whose generalization to $N > 2$ we postpone to future work. Furthermore, by comparing with the exact solutions presented here or those derived in the limit of strong interactions [74, 75] one could verify the performance of the proposed experimental system as a quantum simulator. The system can then be used to reliably study more general regimes where complexity theory might rule out efficient classical solutions. In particular, deviations from the square-well potential will break S_n [but not $SU(N)$] symmetry. This will for example lift the degeneracy of the most antisymmetric spin state (highest energy eigenspace for $U > 0$). Depending on how this degeneracy is lifted, exotic many-body states might arise [76, 77].

Finally, thanks to its high $S_n \times SU(N)$ symmetry, the present system allows one to implement powerful quantum information protocols, such as the density matrix spectrum estimation protocol of Keyl and Werner [78, 79].

Acknowledgments

We thank S. Jordan, J. Haah, J. Preskill, K. Hazzard, G. Campbell, E. Tiesinga, and D. Barker for discussions. This work was supported by NSF IQIM-PFC-1125565, NSF JQI-PFC-0822671, NSF JQI-PFC-1430094, NSF JILA-PFC-1125844, NSF-PIF, NIST, ARO, ARL, ARO-DARPA-OLE, AFOSR, AFOSR MURI, and the Lee A. DuBridge and Gordon and Betty Moore foundations. APK was supported by the Department of Defense through the NDSEG program. MEB and AVG acknowledge the Centro de Ciencias de Benasque Pedro Pascual for hospitality.

[1] I. Bloch, J. Dalibard, and W. Zwerger, Rev. Mod. Phys. **80**, 885 (2008).
[2] I. Bloch, J. Dalibard, and S. Nascimbene, Nature Phys. **8**, 267 (2012).
[3] L. Balents, Nature (London) **464**, 199 (2010).
[4] D. M. Basko, I. L. Aleiner, and B. L. Altshuler, Ann. Phys. **321**, 1126 (2006).
[5] A. Polkovnikov, K. Sengupta, A. Silva, and M. Vengalattore, Rev. Mod. Phys. **83**, 863 (2011).
[6] P. Richerme, Z.-X. Gong, A. Lee, C. Senko, J. Smith, M. Foss-Feig, S. Michalakis, A. V. Gorshkov, and C. Monroe, Nature **511**, 198 (2014).
[7] P. Jurcevic, B. P. Lanyon, P. Hauke, C. Hempel, P. Zoller, R. Blatt, and C. F. Roos, Nature (London) **511**, 202 (2014).
[8] A. Das and B. K. Chakrabarti, Rev. Mod. Phys. **80**, 1061 (2008).
[9] C. Wu, Phys. Rev. Lett. **100**, 200406 (2008).
[10] J. Simon, W. S. Bakr, R. Ma, M. E. Tai, P. M. Preiss, and M. Greiner, Nature (London) **472**, 307 (2011).
[11] S. Pielawa, T. Kitagawa, E. Berg, and S. Sachdev, Phys. Rev. B **83** (2011).
[12] P. Schauß, M. Cheneau, M. Endres, T. Fukuhara, S. Hild, A. Omran, T. Pohl, C. Gross, S. Kuhr, and I. Bloch, Nature (London) **491**, 87 (2012).
[13] L. M. Duan, E. Demler, and M. D. Lukin, Phys. Rev. Lett. **91**, 090402 (2003).
[14] S. Trotzky, P. Cheinet, S. Folling, M. Feld, U. Schnorrberger, A. M. Rey, A. Polkovnikov, E. A. Demler, M. D. Lukin, and I. Bloch, Science **319**, 295 (2008).
[15] T. Fukuhara, P. Schausz, M. Endres, S. Hild, M. Cheneau, I. Bloch, and C. Gross, Nature **502**, 76 (2013).
[16] D. Greif, T. Uehlinger, G. Jotzu, L. Tarruell, and T. Esslinger, Science **340**, 1307 (2013).
[17] S. Hild, T. Fukuhara, P. Schauß, J. Zeiher, M. Knap, E. Demler, I. Bloch, and C. Gross, Phys. Rev. Lett. **113**, 147205 (2014).
[18] R. A. Hart, P. M. Duarte, T.-L. Yang, X. Liu, T. Paiva, E. Khatami, R. T. Scalettar, N. Trivedi, D. A. Huse, and R. G. Hulet, Nature (London) **519**, 211 (2015).
[19] R. C. Brown, R. Wyllie, S. B. Koller, E. A. Goldschmidt, M. Foss-Feig, and J. V. Porto, Science **348**, 540 (2015).
[20] M. Gullans, T. G. Tiecke, D. E. Chang, J. Feist, J. D. Thompson, J. I. Cirac, P. Zoller, and M. D. Lukin, Phys. Rev. Lett. **109**, 235309 (2012).
[21] O. Romero-Isart, C. Navau, A. Sanchez, P. Zoller, and J. I. Cirac, Phys. Rev. Lett. **111**, 145304 (2013).
[22] A. González-Tudela, C. L. Hung, D. E. Chang, J. I. Cirac, and H. J. Kimble, Nature Photon. **9**, 320 (2015).
[23] K. Gibble, Phys. Rev. Lett. **103**, 113202 (2009).
[24] A. M. Rey, A. V. Gorshkov, and C. Rubbo, Phys. Rev. Lett. **103**, 260402 (2009).
[25] Z. Yu and C. J. Pethick, Phys. Rev. Lett. **104**, 010801 (2010).
[26] H. K. Pechkis, J. P. Wrubel, A. Schwettmann, P. F. Griffin, R. Barnett, E. Tiesinga, and P. D. Lett, Phys. Rev. Lett. **111**, 025301 (2013).
[27] C. Deutsch, F. Ramirez-Martinez, C. Lacroûte, F. Reinhard, T. Schneider, J. N. Fuchs, F. Piéchon, F. Laloë, J. Reichel, and P. Rosenbusch, Phys. Rev. Lett. **105**, 020401 (2010).
[28] W. Maineult, C. Deutsch, K. Gibble, J. Reichel, and P. Rosenbusch, Phys. Rev. Lett. **109**, 020407 (2012).
[29] E. L. Hazlett, Y. Zhang, R. W. Stites, K. Gibble, and K. M. O'Hara, Phys. Rev. Lett. **110**, 160801 (2013).
[30] M. J. Martin, M. Bishof, M. D. Swallows, X. Zhang, C. Benko, J. von Stecher, A. V. Gorshkov, A. M. Rey, and J. Ye, Science **341**, 632 (2013).
[31] M. D. Swallows, M. Bishof, Y. Lin, S. Blatt, M. J. Martin, A. M. Rey, and J. Ye, Science **331**, 1043 (2011).
[32] A. P. Koller, M. Beverland, A. V. Gorshkov, and A. M. Rey, Phys. Rev. Lett. **112**, 123001 (2014).
[33] A. V. Gorshkov, M. Hermele, V. Gurarie, C. Xu, P. S. Julienne, J. Ye, P. Zoller, E. Demler, M. D. Lukin, and A. M. Rey, Nature Phys. **6**, 289 (2010).
[34] M. A. Cazalilla, A. F. Ho, and M. Ueda, New J. Phys. **11**, 103033 (2009).
[35] X. Zhang, M. Bishof, S. L. Bromley, C. V. Kraus, M. S. Safronova, P. Zoller, A. M. Rey, and J. Ye, Science **345**, 1467 (2014).
[36] F. Scazza, C. Hofrichter, M. Hofer, P. C. De Groot, I. Bloch, and S. Folling, Nature Phys. **10**, 779 (2014).
[37] G. Pagano, M. Mancini, G. Cappellini, P. Lombardi, F. Schafer, H. Hu, X.-J. Liu, J. Catani, C. Sias, M. Inguscio, et al., Nature Phys. **10**, 198 (2014).
[38] G. Cappellini, M. Mancini, G. Pagano, P. Lombardi, L. Livi, M. Siciliani de Cumis, P. Cancio, M. Pizzocaro, D. Calonico, F. Levi, et al., Phys. Rev. Lett. **113**, 120402 (2014).
[39] A. Sorensen and K. Molmer, Phys. Rev. Lett. **82**, 1971 (1999).
[40] J. W. Britton, B. C. Sawyer, A. C. Keith, C.-C. J. Wang, J. K. Freericks, H. Uys, M. J. Biercuk, and J. J. Bollinger, Nature **484**, 489 (2012).
[41] A. Micheli, G. K. Brennen, and P. Zoller, Nature Phys. **2**, 341 (2006).
[42] R. Barnett, D. Petrov, M. Lukin, and E. Demler, Phys. Rev. Lett. **96**, 190401 (2006).
[43] A. V. Gorshkov, S. R. Manmana, G. Chen, J. Ye, E. Demler, M. D. Lukin, and A. M. Rey, Phys. Rev. Lett. **107**, 115301 (2011).
[44] B. Yan, S. A. Moses, B. Gadway, J. P. Covey, K. R. A. Hazzard, A. M. Rey, D. S. Jin, and J. Ye, Nature (London) **501**, 521 (2013).
[45] A. V. Gorshkov, K. R. A. Hazzard, and A. M. Rey, Mol. Phys. **111**, 1908 (2013).
[46] J. Eisert, M. Friesdorf, and C. Gogolin, Nature Phys. **11**, 124 (2015).
[47] A. Sommer, M. Ku, G. Roati, and M. W. Zwierlein, Nature (London) **472**, 201 (2011).
[48] M. Koschorreck, D. Pertot, E. Vogt, and M. Kohl, Nature Phys. **9**, 405 (2013).
[49] D. M. Greenberger, M. A. Horne, and A. Zeilinger, in 'Bell's Theorem, Quantum Theory, and Conceptions of the Universe', M. Kafatos (Ed.), Kluwer, Dordrecht pp. 69–72 (1989).
[50] J. J. Bollinger, W. M. Itano, D. J. Wineland, and D. J. Heinzen, Phys. Rev. A **54**, R4649 (1996).
[51] R. H. Dicke, Phys. Rev. **93**, 99 (1954).
[52] See Supplemental Material at ??? for the details omitted in the main text.
[53] W. Fulton and J. Harris, *Representation Theory: A First*

Course (Graduate Texts in Mathematics) (Springer, New York, 1991).
[54] A. Alex, M. Kalus, A. Huckleberry, and J. von Delft, J. Math. Phys. **52**, 023507 (2011).
[55] C. A. Sackett, D. Kielpinski, B. E. King, C. Langer, V. Meyer, C. J. Myatt, M. Rowe, Q. A. Turchette, W. M. Itano, D. J. Wineland, et al., Nature (London) **404**, 256 (2000).
[56] M. A. Nielsen and I. L. Chuang, *Quantum Computation and Quantum Information* (Cambridge University Press, Cambridge, 2000).
[57] T. Dutta, M. Mukherjee, and K. Sengupta, Phys. Rev. Lett. **111**, 170406 (2013).
[58] L. I. R. Gil, R. Mukherjee, E. M. Bridge, M. P. A. Jones, and T. Pohl, Phys. Rev. Lett. **112**, 103601 (2014).
[59] B. Olmos, D. Yu, Y. Singh, F. Schreck, K. Bongs, and I. Lesanovsky, Phys. Rev. Lett. **110**, 143602 (2013).
[60] B. J. Bloom, T. L. Nicholson, J. R. Williams, S. L. Campbell, M. Bishof, X. Zhang, W. Zhang, S. L. Bromley, and J. Ye, Nature (London) **506**, 71 (2014).
[61] T. L. Nicholson, S. L. Campbell, R. B. Hutson, G. E. Marti, B. J. Bloom, R. L. McNally, W. Zhang, M. D. Barrett, M. S. Safronova, G. F. Strouse, et al., Nature Commun. **6**, 6896 (2015).
[62] M. M. Boyd, T. Zelevinsky, A. D. Ludlow, S. M. Foreman, S. Blatt, T. Ido, and J. Ye, Science **314**, 1430 (2006).
[63] M. Saffman and K. Molmer, Phys. Rev. Lett. **102**, 240502 (2009).
[64] A. Traverso, R. Chakraborty, Y. N. Martinez de Escobar, P. G. Mickelson, S. B. Nagel, M. Yan, and T. C. Killian, Phys. Rev. A **79**, 060702 (2009).
[65] M. Bishof, M. J. Martin, M. D. Swallows, C. Benko, Y. Lin, G. Quéméner, A. M. Rey, and J. Ye, Phys. Rev. A **84**, 052716 (2011).
[66] A. V. Gorshkov, A. M. Rey, A. J. Daley, M. M. Boyd, J. Ye, P. Zoller, and M. D. Lukin, Phys. Rev. Lett. **102**, 110503 (2009).
[67] H. Aschauer, W. Dur, and H. J. Briegel, Phys. Rev. A **71**, 012319 (2005).
[68] J. Ye, H. J. Kimble, and H. Katori, Science **320**, 1734 (2008).
[69] K. D. Nelson, X. Li, and D. S. Weiss, Nature Phys. **3**, 556 (2007).
[70] Y. N. Martinez de Escobar, P. G. Mickelson, P. Pellegrini, S. B. Nagel, A. Traverso, M. Yan, R. Côté, and T. C. Killian, Phys. Rev. A **78**, 062708 (2008).
[71] K. R. A. Hazzard, V. Gurarie, M. Hermele, and A. M. Rey, Phys. Rev. A **85**, 041604 (2012).
[72] S. Taie, R. Yamazaki, S. Sugawa, and Y. Takahashi, Nature Phys. **8**, 825 (2012).
[73] A. M. Rey, L. Jiang, M. Fleischhauer, E. Demler, and M. D. Lukin, Phys. Rev. A **77**, 052305 (2008).
[74] A. G. Volosniev, D. Petrosyan, M. Valiente, D. V. Fedorov, A. S. Jensen, and N. T. Zinner, Phys. Rev. A **91**, 023620 (2015).
[75] F. Deuretzbacher, D. Becker, J. Bjerlin, S. M. Reimann, and L. Santos, Phys. Rev. A **90**, 013611 (2014).
[76] M. A. Cazalilla and A. M. Rey, Rep. Prog. Phys. **77**, 124401 (2014).
[77] A. M. Rey, A. V. Gorshkov, C. V. Kraus, M. J. Martin, M. Bishof, M. D. Swallows, X. Zhang, C. Benko, J. Ye, N. D. Lemke, et al., Ann. Phys. **340**, 311 (2014).
[78] M. Keyl and R. F. Werner, Phys. Rev. A **64** (2001).
[79] M. E. Beverland et al., in preparation (2015).
[80] For temperatures far from degeneracy, the probability of multiple occupancy will be small. Alternatively, absence of multiple occupancy is guaranteed by Pauli exclusion for nuclear-spin polarized states.